2024 European Control Conference (ECC)
June 25-28, 2024. Stockholm, Sweden

Passivity-Based Pressure Control for Grid-Forming Compressors in Gas Networks

Albertus Johannes Malan[a], Armin Gießler[a], Felix Strehle[a] and Sören Hohmann[a]

***Abstract*— An increase in local renewable gas production will necessitate gas outflows to higher pressure networks to achieve balancing in the future gas networks. We expand on traditional valve-based pressure regulation by introducing a grid-forming compressor unit. This unit incorporates a centrifugal compressor based on the Greitzer model and enables pressure regulation with bi-directional gas flows. Nonlinear controllers are proposed for the valves of the compressor unit, whereas a proportional-integral controller with damping injection is used for the centrifugal compressor. We provide scalar design inequalities for controller which ensure the controlled compressor unit is equilibrium-independent passive (EIP). By showing that the gas pipelines also EIP, we demonstrate the modular and topology-independent stability of the gas network equilibrium in which so-called prosumers may inject or extract gas at any node in the network. The controller and stability results are verified via simulations.**

I. Introduction

CURRENT gas networks are similarly structured as traditional power systems, with high-pressure transmission networks supplying lower pressure regional distribution networks (see [1, p. 51], [2]). This similarity extends to the pressure (vs. voltage) regulation, which must be maintained between upper and lower bounds for safe operation. Unlike in power systems, however, most gas networks have a strict top-down uni-directional supply in which valves are used for pressure regulation.

In future, power-to-gas systems which can inject gas locally are expected to see significant growth. Simultaneously, a reduction in gas demand is being observed, as countries seek to decarbonise [2]. This combination gives rise to situations where the local production outstrips the demand and where gas must therefore either be stored or injected into higher-pressure transmission networks [3, p. 9f.]. However, both options require the addition of compressors to realise the required pressure increases.

Centrifugal compressors, which offer a continuous flow of gas and a high efficiency, are commonly used in gas networks for this purpose [4]. Despite these advantages, these compressors exhibit compressor surge at low flow rates, which can lead to unstable behaviour. Various controllers have been proposed to deal with compressor surge in the literature. In [5], [6], compressor surge is prevented by controlling the speed of the driving machine. This idea is extended in [7], where back-stepping and passivity is employed. In [8], a robust controller using state-feedback linearisation is used alongside a close-coupled valve (CCV) which acts on the unstable compressor dynamics. However, these approaches all assume a constant inlet pressure, restricting their practicality for gas networks where the pressures can vary. More recently, several model predictive control (MPC) solutions for controlling centrifugal compressors have been proposed. In [9] and [10], anti-surge MPCs are used, which ensure robust control of the outlet pressure even under input pressure disturbances. This focus on robust control is extended in [11], where an MPC-based output pressure regulation is achieved for a non-ideal compressor model.

In future gas networks, compressors are required to maintain a desired pressure level in the network while extracting the surplus gas during times of local oversupply. There is thus a need for a *grid-forming compressor unit* which can regulate the pressure with bi-directional gas flows by combining valves and a compressor. However, contrary to the common approach in the literature, this requires a regulation of the compressor inlet pressure. Moreover, since such compressor units represent actively controlled components being added to the gas network, it is imperative that they do not introduce destabilising effects. Thus, the regulation of these compressor units must be robust against constant disturbances and should allow for a modular integration into existing networks while ensuring stability.

Main Contribution: In this paper, we propose: 1) A graph-based gas network model containing grid-forming compressor units which allow pressure regulation with bi-directional gas flows; 2) A controller for the compressor unit which ensures exact pressure regulation at its inlet while preventing compressor surge; 3) Scalar design inequalities ensuring the controlled compressor units are equilibrium-independent passive (EIP).

We also show that gas pipelines are strictly EIP. By combining these results, we prove that the equilibrium of the pressure regulated gas network is asymptotically stable. Due to the EIP-based approach, our results are inherently modular, scalable and robust against constant disturbances and topology changes.

Notation and Preliminaries: Define as a vector $\boldsymbol{a} = (a_k)$ and a matrix $\boldsymbol{A} = (a_{kl})$. Diag$[\cdot]$ creates a (block-)diagonal matrix from the supplied vectors

[a]Institute of Control Systems (IRS), Karlsruhe Institute of Technology (KIT), 76131 Karlsruhe, Germany. E-mail: {albertus.malan, armin.giessler, felix.strehle, soeren.hohmann}@kit.edu.

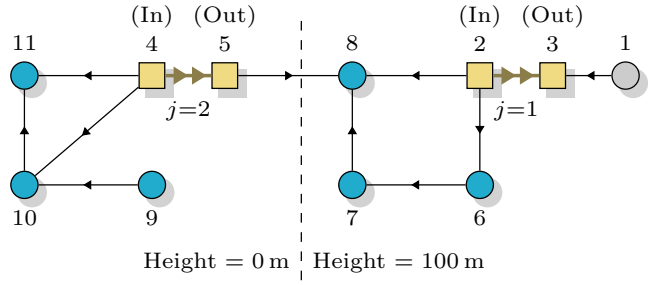

Fig. 1: A gas network comprising nodes ● in $\mathcal{N}_\mathrm{N}$, constant pressure nodes ○ in $\mathcal{N}_\mathrm{S}$, nodes □ in $\mathcal{N}_\mathrm{C}$ adjacent to compressor units ⇾, $j \in \mathcal{E}_\mathrm{C}$, and pipelines with arbitrary directions → in $\mathcal{E}_\mathrm{L}$. The network is divided into two sections situated at different heights.

(or matrices). Let $\boldsymbol{A} \succ 0$ ($\succcurlyeq 0$) denote a positive-(semi)definite matrix. A set $\mathcal{N}$ has the cardinality $|\mathcal{N}|$. For a variable x, we denote its unknown steady state as $\hat{x}$, its error state as $\tilde{x} \coloneqq x - \hat{x}$, and a desired setpoint as x^*. Let $x \equiv 0$ denote that x and all its derivatives are zero for $t \geq 0$. Whenever clear from context, we omit the time dependence of variables. In the gas domain, we denote the absolute pressure as $p > 0$, the constant standard density as $\rho_\mathrm{s} > 0$. The volume flow rate at standard conditions as $q = \dot{m}/\rho_\mathrm{s}$ in sm^3/s is proportional to the mass flow rate $\dot{m}$.

Definition 1: A symmetric matrix is diagonally dominant if $a_{kk} \geq \sum_{l \neq k} |(a_{kl})|, \forall k$. The matrix is strictly diagonally dominant if the inequality holds strictly.

Lemma 2 (Adapted from [12]): A symmetric (strictly) diagonally dominant matrix is (strictly) positive definite.

II. Problem Description

We start by providing a graph-based description of a gas network and introduce its constituent components in Section II-A. Subsequently, in Section II-B, we formulate the considered pressure control problem.

A. System Model

Consider a gas network represented as a finite, directed graph $\mathcal{G} = (\mathcal{N}, \mathcal{E})$ as depicted in Fig. 1, comprising $|\mathcal{N}|$ nodes weakly connected by $|\mathcal{E}|$ edges. The edges are partitioned into two sets: a set of compressor units $\mathcal{E}_\mathrm{C} = \{1, \dots, |\mathcal{E}_\mathrm{C}|\}$, $|\mathcal{E}_\mathrm{C}| \geq 0$, and a set of pipelines $\mathcal{E}_\mathrm{L} = \{|\mathcal{E}_\mathrm{C}| + 1, \dots, |\mathcal{E}_\mathrm{C}| + |\mathcal{E}_\mathrm{L}|\}, |\mathcal{E}_\mathrm{L}| \geq 0$. Furthermore, the nodes are partitioned into three sets: a set of nodes supplying a constant pressure $\mathcal{N}_\mathrm{S} = \{1, \dots, |\mathcal{N}_\mathrm{S}|\}$, $|\mathcal{N}_\mathrm{S}| \geq 1$, a set of nodes situated at the inlet or outlet of a compressor unit $\mathcal{N}_\mathrm{C} = \{|\mathcal{N}_\mathrm{S}| + 1, \dots, |\mathcal{N}_\mathrm{S}| + 2|\mathcal{E}_\mathrm{C}|\}$, and a set of pipe intersections or endpoints $\mathcal{N}_\mathrm{N} = \{|\mathcal{N}_\mathrm{S}| + 2|\mathcal{E}_\mathrm{C}| + 1, \dots, |\mathcal{N}_\mathrm{S}| + 2|\mathcal{E}_\mathrm{C}| + |\mathcal{N}_\mathrm{N}|\}, |\mathcal{N}_\mathrm{N}| \geq 1$. Note that each node in $\mathcal{N}_\mathrm{C}$ is connected to exactly one edge in $\mathcal{E}_\mathrm{C}$. Furthermore, we denote the stacked pressures with $\boldsymbol{p} = (p_n)$, $n \in \mathcal{N}$, and flow rates with $\boldsymbol{q}_\mathrm{L} = (q_i)$, $i \in \mathcal{E}_\mathrm{L}$, where the edge directions denote the positive flow-rate direction. Next, we introduce models for the gas pipelines, valves and centrifugal compressors in the network. Note that p_n is constant for all nodes $n \in \mathcal{N}_\mathrm{S}$.

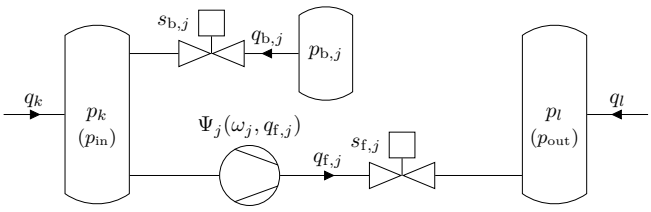

Fig. 2: A compressor unit comprising input and output tanks, a centrifugal compressor, two control valves and a tank with constant pressure $p_{\mathrm{b},j}$.

a) Gas Pipelines: The gas pipelines are modelled using the pi-equivalent structure in [13], where the dynamics of the edges in $\mathcal{E}_\mathrm{L}$ and the nodes in $\mathcal{N}_\mathrm{N}$ are

$$\frac{\rho_\mathrm{s} L_i}{A_i}\dot{q}_i = -\frac{\lambda_{\mathrm{e},i}(q_i)\rho_\mathrm{s}^2 c^2 L_i |q_i| q_i}{2 D_i A_i^2 p_{\mathrm{M},i}} + \boldsymbol{e}_{\mathrm{col},i}^T \boldsymbol{p} - \frac{g L_i \sin(\theta_i)}{c^2} p_{\mathrm{M},i}, \qquad i \in \mathcal{E}_\mathrm{L}, \quad (1)$$

$$V_{\mathrm{eq},n}\dot{p}_n = q_{\mathrm{ex},n} - \boldsymbol{e}_{\mathrm{row},n}^T \boldsymbol{q}_\mathrm{L}, \qquad n \in \mathcal{N}_\mathrm{N}, \quad (2)$$

with the pipeline flow rate $q_i \in \mathbb{R}$, the piecewise constant external flow rate $q_{\mathrm{ex},n} \in \mathbb{R}$, the node pressures $p_n > 0$, and the constant[1] mean pipeline pressure $p_{\mathrm{M},i} > 0$. $L_i, D_i, A_i > 0$ describe the pipe length, diameter and area, and $\theta_i \in [-\frac{\pi}{2}, \frac{\pi}{2}]$ is the pipe inclination angle. Furthermore, $c > 0$ is the speed of sound, $\lambda_{\mathrm{e},i}(\cdot) > 0$ is the equivalent friction factor, and g is the gravitational constant. The row vector $\boldsymbol{e}_{\mathrm{row},n}$ and the column vector $\boldsymbol{e}_{\mathrm{col},i}$ select row n or column i from the *incidence matrix* $\boldsymbol{E}_\mathrm{L} \in \{-1, 0, 1\}^{|\mathcal{N}| \times |\mathcal{E}_\mathrm{L}|}$ comprising the edges in $\mathcal{E}_\mathrm{L}$. The incidence matrix is defined by: $e_{ni} = 1$ if node n is the sink of edge i, $e_{ni} = -1$ if node n is the source of edge i, and $e_{ni} = 0$ otherwise. Additionally,

$$V_{\mathrm{eq},n} = \boldsymbol{e}_{\mathrm{row},n} \operatorname{Diag}\left[\frac{L_i A_i}{2\rho_\mathrm{s} c^2}\right] \boldsymbol{e}_{\mathrm{row},n}^T, \qquad n \in \mathcal{N}, \quad (3)$$

is the constant equivalent capacity in $\mathrm{m}^4\mathrm{s}^2/\mathrm{kg}$ arising from the pipelines connected to a node. Note that gas consumers have $q_{\mathrm{ex},n} < 0$, whereas $q_{\mathrm{ex},n} > 0$ indicate producers injecting gas at a node $n \in \mathcal{N}$.

b) Compressor Units: Consider the compressor unit of an edge $j \in \mathcal{E}_\mathrm{C}$ in Fig. 2 which connects two nodes $k, l \in \mathcal{N}_\mathrm{C}$, where k and l are the source and sink of edge j, respectively. The compressor unit comprises two tanks on the inlet p_k and outlet p_l sides along with a tank with constant pressure[2] $p_{\mathrm{b},j} > p_k$. The operation is split between a backward path with a flow rate $q_{\mathrm{b},j}$ and a forward path with a flow rate $q_{\mathrm{f},j}$. The backward path allows p_k to be increased by an inflow of gas through

[1]This assumption is discussed in [13, Remark 7; Appendix A].

[2]The constant pressure can be maintained, e.g., by using a pressure regulating valve connected to the outlet tank.

a control valve[3] and a pipe of negligible length. The forward path allows p_k to decrease via an outflow of gas through a centrifugal compressor. A CCV is added to the forward path to combat compressor surge. Note that the configuration in Fig. 2 is typical in gas networks, where compressor stations can include multiple stages and operation modes (see [1, p. 42]). We now introduce models for the valves and the compressor which make up the compressor unit.

Control valves are common actuators in gas networks, enabling flow-rate or pressure regulation through a controlled pressure reduction. Regulation is achieved by setting the valve stem position $s_\mathrm{v} \in [0,1]$ to modify its flow area $A_\mathrm{v}(s_\mathrm{v})$. From the standard orifice equation, the flow rate through a valve is [14, p. 49] [4, p. 16]

$$q_\mathrm{v} = C_\mathrm{d} A_\mathrm{v}(s_\mathrm{v}) \sqrt{\frac{2|\Delta p_\mathrm{v}|}{\rho_{\mathrm{v},1}}} \operatorname{sign}(\Delta p_\mathrm{v}), \tag{4}$$

with the differential valve pressure $\Delta p_\mathrm{v} = p_{\mathrm{v},1} - p_{\mathrm{v},2}$, the discharge coefficient C_d, and the inlet density $\rho_{\mathrm{v},1}$. For linear valves with $A_\mathrm{v}(s_\mathrm{v}) = s_\mathrm{v} A_{\mathrm{v},\max}$ and by using the real gas law $p = c^2\rho$ while assuming a constant c, (4) simplifies to

$$q_\mathrm{v} = C_\mathrm{v} s_\mathrm{v} \sqrt{\frac{|\Delta p_\mathrm{v}|}{p_{\mathrm{v},1}}} \operatorname{sign}(\Delta p_\mathrm{v}) \tag{5}$$

$$\iff \Delta p_\mathrm{v} = \frac{p_{\mathrm{v},1}|q_\mathrm{v}|q_\mathrm{v}}{C_\mathrm{v}^2 s_\mathrm{v}^2}, \tag{6}$$

where $C_\mathrm{v} = \sqrt{2} c A_{\mathrm{v},\max} C_\mathrm{d}$ and $\operatorname{sign}(\Delta p_\mathrm{v}) = \operatorname{sign}(q_\mathrm{v})$.

A centrifugal compressor achieves an increase in pressure through a spinning impeller which increases the radial kinetic energy of the gas. This is followed by a diffuser which decelerates the gas and increases the pressure to $\Psi_j(\omega_j, q_{\mathrm{f},j}) p_k > 0$ with (see [5], [15])

$$\Psi_j(\cdot) = \left[1 + \frac{\sigma_j r_{2,j}^2 \omega_j^2 - \frac{r_{1,j}^2}{2}(\omega_j - \alpha_j \rho_\mathrm{s} q_{\mathrm{f},j})^2 - k_{\mathrm{f},j} \rho_\mathrm{s}^2 q_{\mathrm{f},j}^2}{c_\mathrm{p} T_{\mathrm{in},j}}\right]^{\frac{c_\mathrm{p}}{c_\mathrm{p} - c_\mathrm{V}}}, \tag{7}$$

the rotational velocity of the machine ω_j, the flow rate through the compressor $q_{\mathrm{f},j}$, the slip factor $0 < \sigma_j < 1$, the constant zero incidence loss parameter $\alpha_j > 0$, the fluid friction constant $k_{\mathrm{f},j}$, the inlet radius $r_{1,j}$, the impeller radius $r_{2,j}$, the temperature $T_{\mathrm{in},j}$ at the inlet, and the specific heat at constant pressure c_p and constant volume c_V. At low flow rates, the compressor characteristic (7) can exhibit compressor surge which leads to unstable behaviour (see [5]).

The dynamics of the forward path flow rate $q_{\mathrm{f},j}$, comprising the CCV (6) and the compressor (7) are thus

$$\frac{\rho_\mathrm{s} L_{\mathrm{f},j}}{A_{\mathrm{f},j}} \dot{q}_{\mathrm{f},j} = \Psi_j(\omega_j, q_{\mathrm{f},j}) p_k - p_l - \frac{\Psi_j(\omega_j, q_{\mathrm{f},j}) p_k |q_{\mathrm{f},j}| q_{\mathrm{f},j}}{C_\mathrm{v}^2 s_{\mathrm{f},j}^2}, \tag{8a}$$

for $j \in \mathcal{E}_\mathrm{C}$ and where $L_{\mathrm{f},j}, A_{\mathrm{f},j} > 0$ denote the length and cross-sectional area of the forward path pipe, respectively. We assume the pipe friction losses are dominated by the valve losses in (6). The machine driving the compressor is represented by (see [5], [15])

$$J_j \dot{\omega}_j = \tau_j - \sigma_j r_{2,j}^2 \rho_\mathrm{s} q_{\mathrm{f},j} \omega_j - d_j \omega_j, \tag{8b}$$

where $\omega_j \geq 0$ is the rotational velocity, J_j is the rotational inertia, $\sigma_j r_{2,j}^2 \rho_\mathrm{s} q_{\mathrm{f},j} \omega_j$ is the gas pushback torque on the machine, $d_j > 0$ is the rotational friction factor, and the torque $\tau_j \in \mathbb{R}$ is the manipulated variable.

Finally, the dynamics of the tanks are described by

$$V_k \dot{p}_k = q_k + q_{\mathrm{b},j} - q_{\mathrm{f},j}, \qquad q_k = q_{\mathrm{ex},k} - \boldsymbol{e}_{\mathrm{row},k} \boldsymbol{q}_\mathrm{L}, \tag{8c}$$

$$V_l \dot{p}_l = q_l + q_{\mathrm{f},j}, \qquad q_l = q_{\mathrm{ex},l} - \boldsymbol{e}_{\mathrm{row},l} \boldsymbol{q}_\mathrm{L}, \tag{8d}$$

with $0 < p_k \leq \eta p_\mathrm{b}$, $0 < \eta < 1$ and $V_k, V_l > 0$ are the respective constant equivalent capacities, which can include a physical storage tank in addition to the volume from the connecting pipes (3). The upper limit of p_k ensures there is sufficient pressure differential across the valve to perform regulation via s_b.

B. Control Problem

Gas network operators are responsible for *balancing* the in- and outflows of gas in their networks [1, p. 5], which is realised by maintaining the pressure in the network at a desired level. While the specific tolerances can differ greatly, contractually fixed upper and lower bounds for the pressures in a network are mandated[4] for safe operation. In this work, we use the compressor units in Fig. 2 to achieve input pressure regulation along with bi-directional gas flows through the compressor units. Note that we assume suitable pressure setpoints are provided for the control units and that the pressure regulation of the network is feasible, i.e., all components have appropriate dimensions and parameters.

To ensure a scalable, topology-independent and plug-and-play mode of operation while maintaining stability, we use the EIP framework (see [16, p. 24],[17]). By ensuring that each subsystem in the network is either strictly EIP, or EIP and asymptotically stable for a constant input, asymptotic stability can be assured (see [18, Proposition 4.2.3]). For the compressor units, we thus formulate the following control objective:

Objective 1: For each compressor unit $j \in \mathcal{E}_\mathrm{C}$, find $s_{\mathrm{b},j}$, $s_{\mathrm{f},j}$, and τ_j such that $\hat{p}_k = p_k^*$. Furthermore, the controlled compressor unit must be EIP w.r.t. the supply rate[5] $p_k q_k + p_l q_l$ and asymptotically stable if q_k and q_l are constant.

Furthermore, to ensure asymptotic stability for the equilibrium of the entire gas network, we require EIP and asymptotic stability under constant inputs for the graph pipeline nodes (2) and strict EIP for the pipeline edges (1), which we show in Section IV.

[3]The valve with s_b is often referred to as the anti-surge valve or the backflow valve.

[4]E.g., in the German Gas Network Access Ordinance (GasNZV).

[5]The compressor unit supply rate corresponds to the inlet and outlet interaction ports in Fig. 2.

Remark 1: The CCV incurs pressure losses counteracting the pressure rise from the compressor in (8a). To minimise these losses, $s_{\mathrm{f},j}$ should be as open as possible when the compressor is running, while sufficiently damping $q_{\mathrm{f},j}$ to prevent compressor surge at slower flow rates.

III. Compressor Unit Controller

Using the model for a compressor unit $j \in \mathcal{E}_{\mathrm{C}}$, we now propose controllers for the two control valves and the centrifugal compressor such that Objective 1 is met. Specifically, we consider the compressor unit with the dynamics in (8) and with the control inputs $s_{\mathrm{b},j}$, $s_{\mathrm{f},j}$, and τ_j. We then proceed to show that the controlled compressor unit is an input-affine nonlinear system. Finally, we state a condition for the control parameters that ensures the steady state of the controlled compressor has $\hat{p}_k = p_k^*$. For simplicity and clarity in this section, we drop the index j from all parameters and variables, and replace the input and output tank indices with $p_k = p_{\mathrm{in}}$ and $p_l = p_{\mathrm{out}}$.

Since we do not assume a constant input pressure p_{in} (see [5]–[8], [15]) and since the compressor can exhibit compressor surge at low flow rates q_{f}, additional damping is required on the p_{in} and q_{f} states to meet Objective 1 for non-constant input variables. To this end, consider the valve controllers

$$s_{\mathrm{b}} = \left[\xi_{\mathrm{b}}(p_{\mathrm{in}} - p_{\mathrm{in}}^*) + \tfrac{q_{\mathrm{b}}}{C_{\mathrm{v}}}\right]\sqrt{\tfrac{p_{\mathrm{b}}}{|p_{\mathrm{b}} - p_{\mathrm{in}}|}}, \tag{9}$$

$$s_{\mathrm{f}} = \begin{cases} 0, & q_{\mathrm{f}} < 0, \\ \sqrt{\Psi(\cdot)p_{\mathrm{in}}}\ \xi_{\mathrm{f}} q_{\mathrm{f}}^{\frac{3}{4}}, & q_{\mathrm{f}} \geq 0, \end{cases} \tag{10}$$

where $0 < p_{\mathrm{in}}^* \leq \eta p_{\mathrm{b}}$ is the desired input pressure of the compressor unit and $\xi_{\mathrm{b}}, \xi_{\mathrm{f}} > 0$ are control parameters. Increasing s_{b} injects more damping onto the p_{in} state, with a larger ξ_{b} also leading to a slower convergence. Note that the CCV stem position s_{f} closes fully to prevent backflow. Furthermore, s_{f} increases rapidly as q_{f} increases from zero. This allows for greater damping to be injected at lower flow rates. At higher flow rates where compressor surge is not problematic, the CCV opens to reduce the valve pressure loss (see Remark 1). By adjusting ξ_{f}, the position of s_{f} and thus the damping injected onto q_{f} can be set.

Remark 2: In a practical setting, the flow-rate dependent term $q_{\mathrm{b}}/C_{\mathrm{v}}$ in (9) can be generated using an integrator $\dot{\varepsilon}_{\mathrm{b}} = (p_{\mathrm{in}} - p_{\mathrm{in}}^*)/\xi_{\mathrm{bi}}$, $\xi_{\mathrm{bi}} > 0$. This circumvents the need to measure q_{b} and provides robustness against changes in the valve parameter C_{v}.

The centrifugal compressor is regulated using the following PI-like controller

$$\tau = \varepsilon_{\mathrm{c}} + \xi_{\mathrm{p}}(p_{\mathrm{in}} - p_{\mathrm{in}}^*) - \xi_\omega(\omega - \omega_0) - \tfrac{\xi_{\mathrm{p}}\xi_{\mathrm{s}}}{\xi_{\mathrm{i}}} s_{\mathrm{b}}, \tag{11a}$$

$$\dot{\varepsilon}_{\mathrm{c}} = \xi_{\mathrm{i}}(p_{\mathrm{in}} - p_{\mathrm{in}}^*) - \xi_{\mathrm{s}} s_{\mathrm{b}}, \tag{11b}$$

$$\omega_0 = \sqrt{\frac{c_{\mathrm{p}} T_{\mathrm{in}}}{\sigma r_2^2 - \frac{r_1^2}{2}}\left(\Psi_0^{\frac{c_{\mathrm{p}} - c_{\mathrm{V}}}{c_{\mathrm{p}}}} - 1\right)}, \tag{11c}$$

where $\varepsilon_{\mathrm{c}} \in \mathbb{R}$ is an integral term; $\xi_{\mathrm{p}}, \xi_{\mathrm{i}} > 0$ are the proportional and integral gains, respectively; and $\xi_\omega > 0$ injects damping onto the ω state. The dependence of (11a) and (11b) on s_{b} through $\xi_{\mathrm{s}} > 0$ lowers the torque τ when the damping valve controlled by s_{b} (9) is open. Furthermore, a faster start-up of the compressor is achieved using a constant feed-forward term $\omega_0 > 0$ (11c), which is derived from (7) for a chosen pressure ratio $\Psi_0 > 1$ with $q_{\mathrm{f}} \to 0$.

In order to analyse the controlled compressor unit in the sequel, we now formulate its dynamics as an input-affine system by combining the control with the compressor unit. For convenience in the subsequent analysis, we also define

$$z \coloneqq \tfrac{\xi_{\mathrm{p}}}{\xi_{\mathrm{i}}}\varepsilon_{\mathrm{c}} - J\omega, \tag{12}$$

as a transformation for the integral state in (11b).

Proposition 3: Assuming fast dynamics for the backward flow rate q_{b} and a positive forward flow rate $q_{\mathrm{f}} > 0$, the dynamics of the compressor unit (8) controlled using (9)–(11) are

$$\underbrace{\begin{bmatrix} V_{\mathrm{in}}\dot{p}_{\mathrm{in}} \\ V_{\mathrm{out}}\dot{p}_{\mathrm{out}} \\ \frac{\rho_{\mathrm{s}} L_{\mathrm{f}}}{A_{\mathrm{f}}}\dot{q}_{\mathrm{f}} \\ J\dot{\omega} \\ \dot{z} \end{bmatrix}}_{\boldsymbol{Q}_{\mathrm{c}}\dot{\boldsymbol{x}}_{\mathrm{c}}} = \underbrace{\begin{bmatrix} -\frac{C_{\mathrm{v}}\xi_{\mathrm{b}}}{2}(p_{\mathrm{in}} - p_{\mathrm{in}}^*) - q_{\mathrm{f}} \\ q_{\mathrm{f}} \\ \Psi(\cdot)p_{\mathrm{in}} - p_{\mathrm{out}} - \mathcal{R}(\cdot) \\ f_\omega(\cdot) - f_z(\cdot) \\ f_z(\cdot) \end{bmatrix}}_{\boldsymbol{f}_{\mathrm{c}}(\boldsymbol{x}_{\mathrm{c}})} + \underbrace{\begin{bmatrix} q_{\mathrm{in}} \\ q_{\mathrm{out}} \\ 0 \\ 0 \\ 0 \end{bmatrix}}_{\boldsymbol{B}_{\mathrm{c}}\boldsymbol{u}_{\mathrm{c}}}, \tag{13}$$

$$\boldsymbol{y}_{\mathrm{c}} = \underbrace{\begin{bmatrix} 1 & 0 & 0 & 0 & 0 \\ 0 & 1 & 0 & 0 & 0 \end{bmatrix}}_{\boldsymbol{B}_{\mathrm{c}}^T}\boldsymbol{x}_{\mathrm{c}} = \begin{bmatrix} p_{\mathrm{in}} \\ p_{\mathrm{out}} \end{bmatrix}, \tag{14}$$

where $\boldsymbol{x}_{\mathrm{c}}^T = [p_{\mathrm{in}}, p_{\mathrm{out}}, q_{\mathrm{f}}, \omega, z]$, $\boldsymbol{u}_{\mathrm{c}}^T = [q_{\mathrm{in}}, q_{\mathrm{out}}]$ and

$$f_\omega(p_{\mathrm{in}}) \coloneqq \xi_{\mathrm{p}}\left(1 - \tfrac{\xi_{\mathrm{b}}\xi_{\mathrm{s}}}{2\xi_{\mathrm{i}}}\sqrt{\tfrac{p_{\mathrm{b}}}{|p_{\mathrm{b}} - p_{\mathrm{in}}|}}\right)(p_{\mathrm{in}} - p_{\mathrm{in}}^*), \tag{15}$$

$$f_z(q_{\mathrm{f}}, \omega, z) \coloneqq (\xi_\omega + d + \sigma r_2^2 \rho_{\mathrm{s}} q_{\mathrm{f}} - \tfrac{\xi_{\mathrm{i}} J}{\xi_{\mathrm{p}}})\omega + \xi_\omega\omega_0 - \tfrac{\xi_{\mathrm{i}}}{\xi_{\mathrm{p}}} z, \tag{16}$$

$$\mathcal{R}(q_{\mathrm{f}}) \coloneqq \frac{\sqrt{q_{\mathrm{f}}}}{C_{\mathrm{v}}^2 \xi_{\mathrm{f}}^2}. \tag{17}$$

Proof: For the backward flow rate, $\dot{q}_{\mathrm{b}} = 0$. Thus, the valve pressure difference is described by (6). Substituting the valve controller s_{b} (9) into (6) gives

$$p_{\mathrm{b}} - p_{\mathrm{in}} = \tfrac{p_{\mathrm{b}}}{C_{\mathrm{v}}^2 s_{\mathrm{b}}^2}|q_{\mathrm{b}}|q_{\mathrm{b}}, \tag{18a}$$

$$C_{\mathrm{v}}^2 s_{\mathrm{b}}^2 |p_{\mathrm{b}} - p_{\mathrm{in}}| \operatorname{sign}(p_{\mathrm{b}} - p_{\mathrm{in}}) = p_{\mathrm{b}}|q_{\mathrm{b}}|q_{\mathrm{b}}, \tag{18b}$$

$$C_{\mathrm{v}}^2\left[\xi_{\mathrm{b}}(p_{\mathrm{in}} - p_{\mathrm{in}}^*) + \tfrac{q_{\mathrm{b}}}{C_{\mathrm{v}}}\right]^2 = q_{\mathrm{b}}^2, \tag{18c}$$

since $\operatorname{sign}(p_{\mathrm{b}} - p_{\mathrm{in}}) = \operatorname{sign}(q_{\mathrm{b}})$. The trivial solution of (18c) gives $p_{\mathrm{in}} = p_{\mathrm{in}}^*$ and $q_{\mathrm{b}} \in \mathbb{R}$, i.e. any required flow rate is supported when the pressure is at the desired value. By expanding (18c), the solution for $p_{\mathrm{in}} \neq p_{\mathrm{in}}^*$ is found as

$$C_{\mathrm{v}}^2\xi_{\mathrm{b}}^2(p_{\mathrm{in}} - p_{\mathrm{in}}^*)^2 + 2C_{\mathrm{v}}\xi_{\mathrm{b}}(p_{\mathrm{in}} - p_{\mathrm{in}}^*)q_{\mathrm{b}} = 0, \tag{18d}$$

$$-\tfrac{C_{\mathrm{v}}\xi_{\mathrm{b}}}{2}(p_{\mathrm{in}} - p_{\mathrm{in}}^*) = q_{\mathrm{b}}. \tag{18e}$$

Replacing q_b in (8c) with (18e) results in the first state equation in (13). The state equation for p_out in (13) is unchanged from (8d), whereas the dynamics of q_f is obtained by substituting (10) into (8a) and simplifying to obtain $\mathcal{R}(\cdot)$ in (17). Furthermore, substituting τ (11a) and $\varepsilon_\mathrm{c} = \xi_\mathrm{i}/\xi_\mathrm{p}(z + J\omega)$ from (12) into the dynamics of ω (8b) leads to the fourth state equation in (13), with $f_z(\cdot)$ and $f_\omega(\cdot)$ as defined in (15) and (16). Lastly, by constructing

$$\dot{z} = \tfrac{\xi_\mathrm{p}}{\xi_\mathrm{i}}\dot{\varepsilon}_\mathrm{c} - J\dot{\omega} = \xi_\mathrm{p}(p_\mathrm{in} - p_\mathrm{in}^*) - \tfrac{\xi_\mathrm{p}\xi_\mathrm{b}}{\xi_\mathrm{i}} s_\mathrm{b} - J\dot{\omega} = f_z(\cdot), \quad (19)$$

we obtain the dynamics of the transformed state z. ∎

Proposition 3 demonstrates that the controlled compressor unit can be written as a nonlinear input-affine system. Furthermore, the chosen output in (14) corresponds to the interaction port of the pipelines. We now analyse the controlled compressor unit and derive conditions such that the first part of Objective 1 is met, i.e. $\hat{p}_\mathrm{in} = p_\mathrm{in}^*$.

Proposition 4: The steady state of the controlled compressor unit in (13) ensures $\hat{p}_\mathrm{in} = p_\mathrm{in}^*$ if

$$2\xi_\mathrm{i} < \xi_\mathrm{s}\xi_\mathrm{b} \quad \vee \quad 2\xi_\mathrm{i} > \xi_\mathrm{s}\xi_\mathrm{b}\sqrt{\tfrac{1}{1-\eta}}. \quad (20)$$

Proof: The equilibrium state $\hat{p}_\mathrm{in}$ of the system (13) can be derived by considering the steady states $\dot{\omega} = 0$ and $\dot{z} = 0$. Starting from the latter, observe that $\dot{z} = 0 = f_z(\cdot)$, which results in $J\dot{\omega} = 0 = f_\omega(\cdot) - f_z(\cdot) = f_\omega(\cdot)$. From the function definition in (15), we obtain

$$f_\omega(\hat{p}_\mathrm{in}) = 0 \implies \tfrac{2\xi_\mathrm{i}}{\xi_\mathrm{b}\xi_\mathrm{s}} = \sqrt{\tfrac{p_\mathrm{b}}{|p_\mathrm{b} - \hat{p}_\mathrm{in}|}} \quad \vee \quad \hat{p}_\mathrm{in} = p_\mathrm{in}^*. \quad (21)$$

Since $0 < p_\mathrm{in} \leq \eta p_\mathrm{b}$, we observe that

$$1 \leq \sqrt{\tfrac{p_\mathrm{b}}{|p_\mathrm{b} - \hat{p}_\mathrm{in}|}} \leq \sqrt{\tfrac{1}{1-\eta}}. \quad (22)$$

Restricting the control parameters according to (20) thus ensures that $\hat{p}_\mathrm{in} = p_\mathrm{in}^*$ is the only valid solution to (21) and therefore the only valid steady-state pressure for the controlled compressor unit (13). ∎

Remark 3: The controlled dynamics in (13) shows how damping is injected to the system. Specifically, p_in and z receive damping proportional to the respective parameters ξ_b and $\xi_\mathrm{i}/\xi_\mathrm{p}$ (see (16)). Furthermore, the damping of ω is adjusted linearly via ξ_ω in (16), whereas q_f receives nonlinear damping tuned by ξ_f in (17).

IV. Component Passivity & Network Stability

To ensure the desired asymptotic stability for the gas network equilibrium, we now analyse the EIP properties of its constitutive components. To facilitate the subsequent analysis of both the compressor units and the pipelines, we first introduce a useful lemma for establishing the EIP for a class of nonlinear systems, mirroring results in [19]. Thereafter, we analyse the controlled compressor units in Section IV-A and the pipelines in Section IV-B. Finally, we prove the desired asymptotic stability property in Section IV-C.

Lemma 5: Consider the system described by

$$\boldsymbol{Q}\dot{\boldsymbol{x}} = \boldsymbol{f}(\boldsymbol{x}) + \boldsymbol{B}\boldsymbol{u}, \quad \boldsymbol{y} = \boldsymbol{B}^T\boldsymbol{x}, \quad (23)$$

with $\boldsymbol{x} \in \mathcal{X} \subseteq \mathbb{R}^n$, $\boldsymbol{u}, \boldsymbol{y} \in \mathbb{R}^m$, where $\boldsymbol{Q} \succ 0$ is diagonal, and $\boldsymbol{f}\colon \mathcal{X} \to \mathbb{R}^n$ is a class C^1 function. This system is EIP with a storage function $H(\tilde{\boldsymbol{x}}) = \frac{1}{2}\tilde{\boldsymbol{x}}^T\boldsymbol{Q}\tilde{\boldsymbol{x}}$ and a supply rate $\tilde{\boldsymbol{u}}^T\tilde{\boldsymbol{y}}$ if

$$-\nabla\boldsymbol{f}(\boldsymbol{x}) \succcurlyeq 0, \quad \forall\, \boldsymbol{x} \in \mathcal{X}. \quad (24)$$

Furthermore, (23) is strictly EIP if (24) holds strictly.

Proof: Shift (23) to the equilibrium $\hat{\boldsymbol{x}}$ to obtain

$$\boldsymbol{Q}\dot{\tilde{\boldsymbol{x}}} = \boldsymbol{f}(\boldsymbol{x}) - \boldsymbol{f}(\hat{\boldsymbol{x}}) + \boldsymbol{B}\tilde{\boldsymbol{u}}, \quad \tilde{\boldsymbol{y}} = \boldsymbol{B}^T\tilde{\boldsymbol{x}}, \quad (25)$$

where $\boldsymbol{B}\hat{\boldsymbol{u}} = -\boldsymbol{f}(\hat{\boldsymbol{x}})$ describes the steady state of (23). Substitute (25) into the time derivative of $H(\tilde{\boldsymbol{x}})$ to get

$$\dot{H}(\tilde{\boldsymbol{x}}) = \tilde{\boldsymbol{x}}^T(\boldsymbol{f}(\boldsymbol{x}) - \boldsymbol{f}(\hat{\boldsymbol{x}})) + \tilde{\boldsymbol{x}}^T\boldsymbol{B}\tilde{\boldsymbol{u}}, \quad (26)$$

$$\dot{H}(\tilde{\boldsymbol{x}}) \leq \tilde{\boldsymbol{u}}^T\tilde{\boldsymbol{y}} \impliedby \tilde{\boldsymbol{x}}^T(\boldsymbol{f}(\boldsymbol{x}) - \boldsymbol{f}(\hat{\boldsymbol{x}})) \leq 0, \forall\, \boldsymbol{x} \in \mathcal{X}. \quad (27)$$

Thus, (27) is met if $-\boldsymbol{f}(\boldsymbol{x})$ is monotone (see [20, Definition 12.1]), which can be determined using (24) [20, Proposition 12.3]. Furthermore, strict inequalities in (24) and thus in (27) yield a strictly EIP system. ∎

A. Compressor Unit Passivity

Having verified the first part of Objective 1 through Proposition 4, we now derive conditions for the EIP and the asymptotic stability of the controlled compressor units in the following theorem and proposition. Note that we again drop index j and replace the input and output indices with $p_k = p_\mathrm{in}$ and $p_l = p_\mathrm{out}$ in this subsection.

Theorem 6: The controlled compressor unit in (13) and (14) is EIP with the storage function

$$H_\mathrm{c}(\tilde{\boldsymbol{x}}_\mathrm{c}) = \tfrac{1}{2}\tilde{\boldsymbol{x}}_\mathrm{c}^T\boldsymbol{Q}_\mathrm{c}\tilde{\boldsymbol{x}}_\mathrm{c}, \quad (28)$$

and the supply rate $\tilde{\boldsymbol{u}}_\mathrm{c}^T\tilde{\boldsymbol{y}}_\mathrm{c} = \tilde{q}_\mathrm{in}\tilde{p}_\mathrm{in} + \tilde{q}_\mathrm{out}\tilde{p}_\mathrm{out}$ if (20) holds along with the following inequalities

$$0 \leq C_\mathrm{v}\xi_\mathrm{b} - |1-\Psi| - \xi_\mathrm{p}\gamma, \quad (29a)$$

$$0 \leq 2(\nabla_{q_\mathrm{f}}\mathcal{R} - p_\mathrm{in}\nabla_{q_\mathrm{f}}\Psi) - |1-\Psi| - \left|\sigma r_2^2\rho_\mathrm{s}\omega - p_\mathrm{in}\nabla_\omega\Psi\right| - \sigma r_2^2\rho_\mathrm{s}\omega, \quad (29b)$$

$$0 \leq (\xi_\omega + d + \sigma r_2^2\rho_\mathrm{s}q_\mathrm{f} - \tfrac{J\xi_\mathrm{i}}{\xi_\mathrm{p}}) - \xi_\mathrm{p}\gamma - \left|\sigma r_2^2\rho_\mathrm{s}\omega - p_\mathrm{in}\nabla_\omega\Psi\right| - \tfrac{\xi_\mathrm{i}}{\xi_\mathrm{p}}, \quad (29c)$$

$$0 \leq (1+J)\tfrac{2\xi_\mathrm{i}}{\xi_\mathrm{p}} - \sigma r_2^2\rho_\mathrm{s}(\omega + q) - \xi_\omega - d, \quad (29d)$$

for all $0 < p_\mathrm{in} \leq \eta p_\mathrm{b}$, $0 < q_\mathrm{f} \leq q_\mathrm{fmax}$, $0 \leq \omega \leq \omega_\mathrm{max}$, $0 < p_\mathrm{in}^* \leq \eta p_\mathrm{b}$, and where

$$\nabla_{q_\mathrm{f}}\Psi = \tfrac{1}{(c_\mathrm{p} - c_\mathrm{V})T_\mathrm{in}}\left[\alpha r_1^2\rho_\mathrm{s}\omega - (r_1^2\alpha^2 + 2k_\mathrm{f})\rho_\mathrm{s}q_\mathrm{f}\right]\Psi^{\frac{c_\mathrm{V}}{c_\mathrm{p}}}, \quad (30)$$

$$\nabla_\omega\Psi = \tfrac{1}{(c_\mathrm{p} - c_\mathrm{V})T_\mathrm{in}}\left[(2\sigma r_2^2 - r_1^2)\omega + r_1^2\alpha\rho_\mathrm{s}q_\mathrm{f}\right]\Psi^{\frac{c_\mathrm{V}}{c_\mathrm{p}}}, \quad (31)$$

$$\nabla_{q_\mathrm{f}}\mathcal{R} = \frac{1}{2C_\mathrm{v}^2\xi_\mathrm{f}^2\sqrt{q_\mathrm{f}}}, \quad (32)$$

$$\gamma = \max\left\{\left|1 - \tfrac{\xi_\mathrm{s}\xi_\mathrm{b}(2-\eta)}{4\xi_\mathrm{i}}\right|, \left|1 - \tfrac{\xi_\mathrm{s}\xi_\mathrm{b}(2-\eta)}{4\xi_\mathrm{i}(1-\eta)^{\frac{3}{2}}}\right|\right\}. \quad (33)$$

Proof: By Lemma 5, the compressor unit is EIP if $-\nabla \boldsymbol{f}_{\mathrm{c}}(\boldsymbol{x}_{\mathrm{c}}) \succcurlyeq 0$ for all $\boldsymbol{x}_{\mathrm{c}} \in \mathcal{X}_{\mathrm{c}}$, with

$$\nabla \boldsymbol{f}_{\mathrm{c}} = \begin{bmatrix} -\frac{1}{2}C_{\mathrm{v}}\xi_{\mathrm{b}} & 0 & -1 & 0 & 0 \\ 0 & 0 & 1 & 0 & 0 \\ \Psi & -1 & p_{\mathrm{in}}\nabla_{q_{\mathrm{f}}}\Psi - \nabla_{q_{\mathrm{f}}}\mathcal{R} & p_{\mathrm{in}}\nabla_{\omega}\Psi & 0 \\ \nabla_{p_{\mathrm{in}}} f_{\omega} & 0 & -\nabla_{q_{\mathrm{f}}} f_z & -\nabla_{\omega} f_z & -\nabla_z f_z \\ 0 & 0 & \nabla_{q_{\mathrm{f}}} f_z & \nabla_{\omega} f_z & \nabla_z f_z \end{bmatrix}. \tag{34}$$

Since matrix definiteness is defined for symmetric matrices, $-\nabla \boldsymbol{f}_{\mathrm{c}}(\boldsymbol{x}_{\mathrm{c}}) \succcurlyeq 0$ is equivalent to (35) at the bottom of the page. The matrix inequality in (35) can be verified using diagonal dominance (see Lemma 2). This yields

$$0 \leq C_{\mathrm{v}}\xi_{\mathrm{b}} - |1-\Psi| - |\nabla_{p_{\mathrm{in}}} f_{\omega}|, \tag{36a}$$

$$0 \leq 2(\nabla_{q_{\mathrm{f}}}\mathcal{R} - p_{\mathrm{in}}\nabla_{q_{\mathrm{f}}}\Psi) - |1-\Psi| - |\nabla_{q_{\mathrm{f}}} f_z - p_{\mathrm{in}}\nabla_{\omega}\Psi| - |\nabla_{q_{\mathrm{f}}} f_z|, \tag{36b}$$

$$0 \leq 2\nabla_{\omega} f_z - |\nabla_{p_{\mathrm{in}}} f_{\omega}| - |\nabla_{q_{\mathrm{f}}} f_z - p_{\mathrm{in}}\nabla_{\omega}\Psi| - |\nabla_z f_z - \nabla_{\omega} f_z|, \tag{36c}$$

$$0 \leq -2\nabla_z f_z - |\nabla_{q_{\mathrm{f}}} f_z| - |\nabla_z f_z - \nabla_{\omega} f_z|. \tag{36d}$$

Observe from (15), along with γ in (33), that

$$\begin{aligned} |\nabla_{p_{\mathrm{in}}} f_{\omega}| &= \xi_{\mathrm{p}} \left| 1 - \tfrac{\xi_{\mathrm{s}}\xi_{\mathrm{b}}}{4\xi_{\mathrm{i}}} \sqrt{\tfrac{p_{\mathrm{b}}}{|p_{\mathrm{b}} - p_{\mathrm{in}}|}} \left(2 + \tfrac{p_{\mathrm{in}} - p_{\mathrm{in}}^*}{|p_{\mathrm{b}} - p_{\mathrm{in}}|} \right) \right| \\ &= \xi_{\mathrm{p}} \left| 1 - \tfrac{\xi_{\mathrm{s}}\xi_{\mathrm{b}}}{4\xi_{\mathrm{i}}} \sqrt{\tfrac{p_{\mathrm{b}}}{|p_{\mathrm{b}} - p_{\mathrm{in}}|}} \cdot \tfrac{2p_{\mathrm{b}} - p_{\mathrm{in}} - p_{\mathrm{in}}^*}{|p_{\mathrm{b}} - p_{\mathrm{in}}|} \right| \\ &\leq \xi_{\mathrm{p}}\gamma, \end{aligned} \tag{37}$$

for all valid p_{in} and p_{in}^*.[6] Substituting (37) along with the derivates of f_{ω} and f_z into (36) and simplifying yields conditions (29). ∎

Proposition 7: The controlled compressor unit in Proposition 3 with $\tilde{\boldsymbol{u}}_{\mathrm{c}} = \boldsymbol{0}$ is asymptotically stable if the conditions in (29) hold strictly.

Proof: If (29) hold strictly, then there is an $\epsilon > 0$ such that

$$-(\nabla \boldsymbol{f}_{\mathrm{c}} + \nabla \boldsymbol{f}_{\mathrm{c}}^T) \succcurlyeq \mathrm{Diag}[(\epsilon, 0, \epsilon, \epsilon, \epsilon)]. \tag{38}$$

For constant inputs $\tilde{\boldsymbol{u}}_{\mathrm{c}} = \boldsymbol{0}$, the storage function H_{c} is then a Lyapunov function which ensures asymptotic convergences of the states $\tilde{p}_{\mathrm{in}}$, $\tilde{q}_{\mathrm{f}}$, $\tilde{\omega}$ and $\tilde{z}$ through (38). Asymptotic stability of $\tilde{p}_{\mathrm{out}}$ can then be established using LaSalle's invariance principle, by which $\dot{H}_{\mathrm{c}} \equiv 0$ reduces (13) to $V_{\mathrm{in}}\dot{\tilde{p}}_{\mathrm{in}} = 0$. Moreover, since the error variable $\tilde{p}_{\mathrm{in}} = p_{\mathrm{in}} - \hat{p}_{\mathrm{in}}$ is shifted to the equilibrium $\hat{p}_{\mathrm{in}}$ such that $\tilde{p}_{\mathrm{in}} = 0$ if $\dot{\tilde{p}}_{\mathrm{in}} \equiv 0$, it is verified that $\lim_{t\to\infty} \tilde{\boldsymbol{x}}_{\mathrm{c}} = \boldsymbol{0}$ if $\tilde{\boldsymbol{u}}_{\mathrm{c}} = \boldsymbol{0}$. ∎

[6] $\nabla_{p_{\mathrm{in}}} f_{\omega}$ has a maximum at ($p_{\mathrm{in}} = 0$, $p_{\mathrm{in}}^* = \eta p_{\mathrm{b}}$) and a minimum at ($p_{\mathrm{in}} = \eta p_{\mathrm{b}}$, $p_{\mathrm{in}}^* = 0$), which constitutes the options for γ in (33).

Remark 4: To test the conditions in Theorem 6, note that (29a) simply needs to hold for the extremes of $\Psi(\cdot)$, whereas (29d) simply needs to hold for $\omega_{\max}$ and q_{fmax}. Furthermore, although (29b) and (29c) are arduous to analyse analytically, these scalar inequalities can easily be verified using constrained optimisation methods.

B. Pipeline Passivity

As discussed in Section II-B, the nodes and edges of the pipeline must also exhibit EIP properties. Consider therefore the nodes $n \in \mathcal{N}_{\mathrm{N}}$ with (2), the input $\tilde{q}_n = -\boldsymbol{e}_{\mathrm{row},n}^T \tilde{\boldsymbol{q}}_{\mathrm{L}}$, output $\tilde{p}_n$, and storage function

$$H_{\mathrm{N},n}(\tilde{p}_n) = \tfrac{V_{\mathrm{eq},n}}{2}\tilde{p}_n^2, \tag{39}$$

which can directly be seen to be EIP with a supply rate $\tilde{q}_n\tilde{p}_n$. Furthermore, if $q_{\mathrm{ex},n}$ is constant, then the node dynamics (2) are asymptotically stable by a similar argumentation as in the proof of Proposition 7. For the pipeline edge dynamics, on the other hand, we derive the following strict EIP result.

Proposition 8: The pipeline edge dynamics in (1) with a constant mean pressure $p_{\mathrm{M},i}$ and the input-output pair $(\boldsymbol{e}_{\mathrm{col},i}^T\tilde{\boldsymbol{p}}, \tilde{q}_i)$ are strictly EIP with a storage function

$$H_{\mathrm{L},i}(\tilde{q}_i) = \tfrac{\rho_{\mathrm{s}} L_i}{2A_i}\tilde{q}_i^2, \quad i \in \mathcal{E}_{\mathrm{L}}, \tag{40}$$

and a supply rate $\boldsymbol{e}_{\mathrm{col},i}^T\tilde{\boldsymbol{p}}\tilde{q}_i$.

Proof: Eq. (1) has the form (23), with $Q_{\mathrm{L},i} = \rho_{\mathrm{s}} L_i / A_i$, the input $\boldsymbol{e}_{\mathrm{col},i}^T\boldsymbol{p}$ and

$$\begin{aligned} f_{\mathrm{L},i}(q_i) &= -\frac{\lambda_{\mathrm{e},i}(q_i)\rho_{\mathrm{s}}^2 c^2 L_i |q_i| q_i}{2D_i A_i^2 p_{\mathrm{M},i}} - \frac{g L_i \sin(\theta_i)}{c^2} p_{\mathrm{M},i} \\ &= -\phi_i \lambda_{\mathrm{e},i}(q_i)|q_i|q_i - \tfrac{g L_i \sin(\theta_i)}{c^2} p_{\mathrm{M},i}. \end{aligned} \tag{41}$$

Strict EIP is then assured by Lemma 5 if $-\nabla_{q_i} f_{\mathrm{L},i} > 0$. However, this involves computing the derivative of the $\lambda_{\mathrm{e},i}(\cdot)$ which is non-trivial for turbulent or transitional flow. Nevertheless, strict monotonicity of $f_{\mathrm{L},i}(\cdot)$ can be investigated by looking at the rates at which $\lambda_{\mathrm{e},i}(\cdot)$ decreases and $|q_i|q_i$ increases. The slowest rate of increase of $|q_i|q_i$ occurs for a small q_i. Furthermore, it is well known that the fastest decrease of $\lambda_{\mathrm{e},i}(\cdot)$ takes place for laminar flow (see the log-log Moody diagram [14, p. 60], where q_i is directly proportional to the Reynolds number). Thus, it is sufficient to evaluate $\nabla_{q_i} f_{\mathrm{L},i}$ for laminar flow, where $\lambda_{\mathrm{e},i}(q_i) = \zeta_i |q_i|^{-1}$, with the proportionality factor $\zeta_i > 0$ (see [13, Eq. (7)]). This yields the lower bound

$$-\nabla_{q_i} f_{\mathrm{L},i} \geq \phi_i \zeta_i > 0, \tag{42}$$

which verifies Lemma 5. ∎

$$-(\nabla \boldsymbol{f}_{\mathrm{c}} + \nabla \boldsymbol{f}_{\mathrm{c}}^T) = \begin{bmatrix} C_{\mathrm{v}}\xi_{\mathrm{b}} & 0 & 1-\Psi & -\nabla_{p_{\mathrm{in}}} f_{\omega} & 0 \\ 0 & 0 & 0 & 0 & 0 \\ 1-\Psi & 0 & 2(\nabla_{q_{\mathrm{f}}}\mathcal{R} - p_{\mathrm{in}}\nabla_{q_{\mathrm{f}}}\Psi) & \nabla_{q_{\mathrm{f}}} f_z - p_{\mathrm{in}}\nabla_{\omega}\Psi & -\nabla_{q_{\mathrm{f}}} f_z \\ -\nabla_{p_{\mathrm{in}}} f_{\omega} & 0 & \nabla_{q_{\mathrm{f}}} f_z - p_{\mathrm{in}}\nabla_{\omega}\Psi & 2\nabla_{\omega} f_z & \nabla_z f_z - \nabla_{\omega} f_z \\ 0 & 0 & -\nabla_{q_{\mathrm{f}}} f_z & \nabla_z f_z - \nabla_{\omega} f_z & -2\nabla_z f_z \end{bmatrix} \succcurlyeq 0 \tag{35}$$

TABLE I: Compressor Unit Parameters

$r_{1,j} = 79.5\,\text{mm}$	$r_{2,j} = 135\,\text{mm}$	$\alpha_j = 1181.7$
$k_{\text{f},j} = 10^5\,\text{m}^2/\text{kg}^2$	$C_{\text{v},j} = 1.36\,\text{m}^3/\text{s}$	$\sigma_j = 0.95$
$q_{\text{fmax},j} = 12\,\text{m}^3/\text{s}$	$p_{\text{b},j} = 1.5\,\text{bar}$	$\eta_j = 0.92$
$\omega_{\text{max},j} = 3 \cdot 10^4\,\text{rpm}$	$L_j = 5\,\text{m}$	$D_j = 0.05\,\text{m}$
$d_j = 0.01\,\text{N m s/rad}$	$J_j = 0.9\,\text{kgm}^2$	

TABLE II: Rounded Line Lengths

Line	km	Line	km	Line	km	Line	km
1–3	5.00	2–6	2.93	2–8	2.79	4–10	2.68
4–11	1.25	5–8	1.75	6–7	1.25	7–8	1.52
9–10	1.67	10–11	1.90				

C. Gas Network Stability

Using the established EIP and asymptotic stability results from Theorem 6, Proposition 7 and Proposition 8, we now demonstrate the asymptotic stability of the gas network equilibrium.

Theorem 9: Consider a gas network $\mathcal{G} = (\mathcal{N}, \mathcal{E})$, $\mathcal{N} = \mathcal{N}_\text{N} \cup \mathcal{N}_\text{C} \cup \mathcal{N}_\text{S}$, $\mathcal{E} = \mathcal{E}_\text{C} \cup \mathcal{E}_\text{L}$, which comprises (1), (2), (13), and where p_n is constant for $n \in \mathcal{N}_\text{S}$. The gas network equilibrium characterised by $\hat{p}_k = p_k^*$, for $k \in \mathcal{N}_\text{C}$ and k the source of an edge $j \in \mathcal{E}_\text{C}$, is asymptotically stable if the conditions of Theorem 6 and Proposition 7 hold for each compressor unit.

Proof: Consider the pipeline and compressor interconnections described by (1), (2), and (13) shifted to the equilibrium, i.e. with $\tilde{q}_{\text{ex},n} = 0$, $n \in \mathcal{N}_\text{N} \cup \mathcal{N}_\text{C}$:

$$\begin{bmatrix} \tilde{\boldsymbol{u}}_\text{N} \\ \tilde{\boldsymbol{u}}_\text{C} \\ \tilde{\boldsymbol{u}}_\text{S} \\ \tilde{\boldsymbol{u}}_\text{L} \end{bmatrix} = \begin{bmatrix} \boldsymbol{0} & \boldsymbol{0} & \boldsymbol{0} & -\boldsymbol{E}_\text{N} \\ \boldsymbol{0} & \boldsymbol{0} & \boldsymbol{0} & -\boldsymbol{E}_\text{C} \\ \boldsymbol{0} & \boldsymbol{0} & \boldsymbol{0} & -\boldsymbol{E}_\text{S} \\ \boldsymbol{E}_\text{N}^T & \boldsymbol{E}_\text{C}^T & \boldsymbol{E}_\text{S}^T & \boldsymbol{0} \end{bmatrix} \begin{bmatrix} \tilde{\boldsymbol{y}}_\text{N} \\ \tilde{\boldsymbol{y}}_\text{C} \\ \tilde{\boldsymbol{y}}_\text{S} \\ \tilde{\boldsymbol{y}}_\text{L} \end{bmatrix}, \tag{43}$$

where $\tilde{\boldsymbol{u}}_\text{C}$ and $\tilde{\boldsymbol{y}}_\text{C}$ are the stacked vectors of $\tilde{\boldsymbol{u}}_{\text{c},j}$ and $\tilde{\boldsymbol{y}}_{\text{c},j}$ for $j \in \mathcal{E}_\text{C}$, and where $\boldsymbol{E}_\text{N}$, $\boldsymbol{E}_\text{C}$ and $\boldsymbol{E}_\text{S}$ stack the vectors $\boldsymbol{e}_{\text{row},n}$ for $n \in \mathcal{N}_\text{N}$, $n \in \mathcal{N}_\text{C}$, and $n \in \mathcal{N}_\text{S}$, respectively. Since each of the systems described by the input-output ports $(\tilde{\boldsymbol{u}}_\text{N}, \tilde{\boldsymbol{y}}_\text{N})$, $(\tilde{\boldsymbol{u}}_\text{C}, \tilde{\boldsymbol{y}}_\text{C})$ and $(\tilde{\boldsymbol{u}}_\text{L}, \tilde{\boldsymbol{y}}_\text{L})$ is EIP and since $p_n = const.$, $n \in \mathcal{N}_\text{S}$, ensures that $\tilde{\boldsymbol{y}}_\text{S} = 0$, the gas network equilibrium is stable [16, Theorem 3.1] with a combined Lyapunov function $H = H_{\text{N},n} + H_{\text{c},j} + H_{\text{L},i}$, with $n \in \mathcal{N}_\text{N}$, $j \in \mathcal{E}_\text{C}$, $i \in \mathcal{E}_\text{L}$. Furthermore, since the edges with the input-output port $(\tilde{\boldsymbol{u}}_\text{L}, \tilde{\boldsymbol{y}}_\text{L})$ are strictly EIP, and since the remaining systems are asymptotically stable for constant inputs $\tilde{\boldsymbol{u}}_\text{N} = \boldsymbol{0}$, $\tilde{\boldsymbol{u}}_\text{C} = \boldsymbol{0}$ and $\tilde{\boldsymbol{u}}_\text{S} = \boldsymbol{0}$, the gas network equilibrium is asymptotically stable [18, Proposition 4.2.3]. Finally, from Proposition 4, the gas network equilibrium has $\hat{p}_k = p_k^*$, for $k \in \mathcal{N}_\text{C}$ and k the source of an edge $j \in \mathcal{E}_\text{C}$. ■

V. Simulation

We now demonstrate our results in a MATLAB/SIMULINK simulation using SIMSCAPE components. To this end, consider the 11-node network in Fig. 1 with two compressor units $j \in \{1, 2\}$. The compressor unit parameters are given in Table I and the pipeline lengths in Table II. The tank capacities of the compressors are taken as the pipeline capacities expressed in (3). The pipelines all have a diameter of $D_i = 0.15\,\text{m}$, except for the pipe connecting Nodes 1 and 3, which supplies the entire network, where the pipe diameter is $0.2\,\text{m}$. The gas properties are taken from [13, Table 1]. The control parameters given in Table III are designed such that the conditions in Theorem 6 and Proposition 7 hold for the compressor unit in SI units.

The simulation starts with $p_n = 1.5\,\text{bar}$, $n \in \{1, 3\}$, and $p_n = 1.2\,\text{bar}$, $n \in \mathcal{N} \setminus \{1, 3\}$. The loads are set to $q_{\text{ex},n} = -0.02\,\text{sm}^3/\text{s}$, $n \in \mathcal{N}_\text{N} \cup \{2, 4\}$, and $0\,\text{sm}^3/\text{s}$ at the other nodes. The setpoint $p_4^* = 1.1\,\text{bar}$ is kept constant constant during the simulation, whereas $p_2^* = 1.2\,\text{bar}$ initially, $p_2^* = 1.15\,\text{bar}$ for $200\,\text{s} \leq t < 400\,\text{s}$,

TABLE III: Controller Parameters

Valves (9), (10)	$\xi_{\text{b},j} = 5$	$\xi_{\text{f},j} = 0.0053$	
Compressors (11)	$\xi_{\text{p},j} = 10^{-5}$	$\xi_{\omega,j} = 640$	$\xi_{\text{s},j} = 5 \cdot 10^4$
	$\xi_{\text{i},j} = 20$	$\Psi_{0,j} = 1.5$	

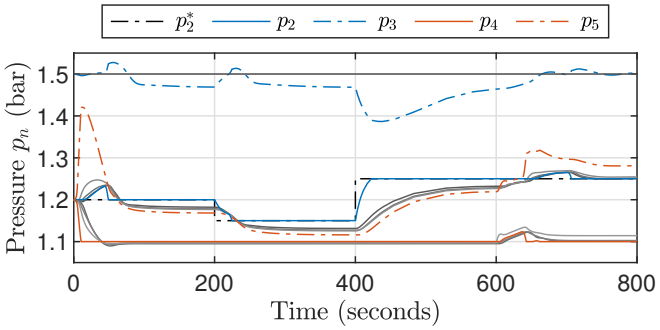

Fig. 3: Node pressures p_n for $n \in \mathcal{N}$.

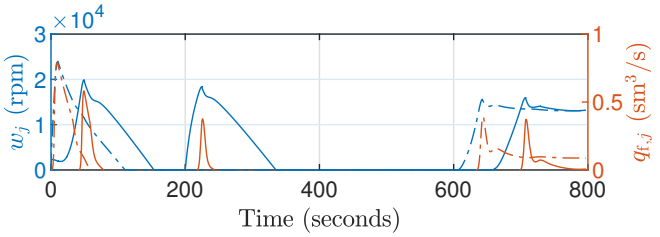

Fig. 4: Compressor angular velocities ω_j and forward flow rates $q_{\text{f},j}$ for $j = 1$ (solid) and $j = 2$ (dash dotted).

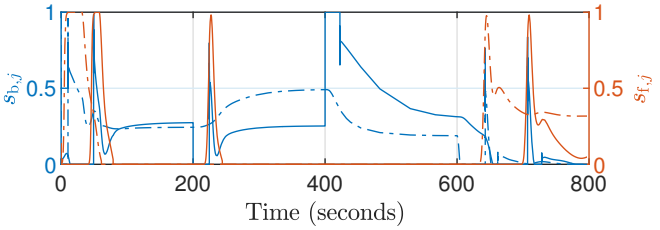

Fig. 5: Stem positions $s_{\text{b},j}$ and $s_{\text{f},j}$ for $j = 1$ (solid) and $j = 2$ (dash dotted).

and $p_2^* = 1.25\,\text{bar}$ for $t \geq 400\,\text{s}$. Finally, the flow rate $q_{\text{ex},11} = 0.148\,\text{sm}^3/\text{s}$ is set for $t \geq 600\,\text{s}$, representing an injection of gas at Node 11. After $t = 600\,\text{s}$, there is thus an oversupply of $\sum_{n\in\mathcal{N}} q_{\text{ex},n} = 0.008\,\text{sm}^3/\text{s}$ which must flow into Node 1 at steady state.[7]

The node pressures in Fig. 3 show that both compressors regulate of their inlet pressures p_2 and p_4 to the desired setpoints, irrespective of the gas flow direction. The compressor activity is shown in Fig. 4, where it can be seen that a sufficient speed must be reached before the forward flow rate increases. Furthermore, we note how the periods of activity in Fig. 4 (see $q_{\text{f},j}$ specifically) correspond to increases in the outlet pressures p_3 and p_5 in Fig. 3, indicating gas being moved to those nodes. This also explains the behaviour after $t = 600\,\text{s}$, where excess gas is injected at Node 11. As the pressures on the left-hand side of the network in Fig. 1 slowly rise, compressor $j = 2$ starts up and moves the excess gas to Node 5. This causes the pressures in the right-hand side of the network to rise, causing compressor $j = 1$ to start a short while later. Finally, the control valve stem positions in Fig. 5 show how both valves in a compressor unit work together to ensure stability, especially in the transient regions. Notice that the CCV with s_{f} opens fully for large flow rates as per Remark 1, minimising the valve pressure losses when there is no risk of compressor surge.

VI. Conclusion

In this paper, we proposed a graph-based gas network model with dynamical pipelines and compressor units which achieves balancing through pressure regulation with bi-directional gas flows. We presented a controller that regulates the inlet pressure of the compressor unit to a desired steady state. By showing that the controlled compressor units are equilibrium-independent passive (EIP) and combining them with strictly EIP pipelines, we verified the asymptotic stability of the desired operating point of the entire network. The stability results are modular, scalable and topology-independent. Future work includes using the pressure setpoints of the controlled compressor units along with higher level controllers to achieve secondary or tertiary control objectives.

References

[1] T. Koch, B. Hiller, M. E. Pfetsch, and L. Schewe, *Evaluating Gas Network Capacities*. Philadelphia, PA: Society for Industrial and Applied Mathematics, 2015.

[2] M. Qadrdan, R. Fazeli, N. Jenkins, G. Strbac, and R. Sansom, "Gas and electricity supply implications of decarbonising heat sector in GB," *Energy*, vol. 169, pp. 50–60, 2019.

[3] European Commission, Directorate-General for Energy, K. Sardi, A. De Vita, and P. Capros, *The role of gas DSOs and distribution networks in the context of the energy transition*. Publications Office, 2020.

[4] M. Qadrdan, M. Abeysekera, J. Wu, N. Jenkins, and B. Winter, *The Future of Gas Networks*, 1st ed. Cham: Springer, 2020.

[7] $q_{\text{ex},11}$ is chosen so that compressor $j = 1$ must operate at a steady-state flow rate where compressor surge normally occurs.

[5] J. Gravdahl and O. Egeland, "Centrifugal compressor surge and speed control," *IEEE Trans. Control Syst. Technol.*, vol. 7, no. 5, pp. 567–579, 1999.

[6] J. T. Gravdahl, O. Egeland, and S. O. Vatland, "Drive torque actuation in active surge control of centrifugal compressors," *Automatica*, vol. 38, no. 11, pp. 1881–1893, 2002.

[7] B. Bøhagen and J. T. Gravdahl, "Active surge control of compression system using drive torque," *Automatica*, vol. 44, no. 4, pp. 1135–1140, 2008.

[8] C. J. Backi, J. T. Gravdahl, and S. Skogestad, "Robust control of a two-state Greitzer compressor model by state-feedback linearization," in *Proc. IEEE Conf. Control Appl. (CCA)*, 2016, pp. 1226–1231.

[9] A. Cortinovis, H. Ferreau, D. Lewandowski, and M. Mercangöz, "Experimental evaluation of mpc-based anti-surge and process control for electric driven centrifugal gas compressors," *J. of Process Control*, vol. 34, pp. 13–25, 2015.

[10] T. Bentaleb, A. Cacitti, S. De Franciscis, and A. Garulli, "Model predictive control for pressure regulation and surge prevention in centrifugal compressors," in *Proc. Eur. Control Conf. (ECC)*, 2015, pp. 3346–3351.

[11] R. L. Meira, M. A. Martins, R. A. Kalid, and G. M. Costa, "Implementable MPC-based surge avoidance nonlinear control strategies for non-ideally modeled natural gas compression systems," *J. Natural Gas Sci. Eng.*, vol. 102, p. 104573, 2022.

[12] J. C. Willems, "Lyapunov functions for diagonally dominant systems," *Automatica*, vol. 12, no. 5, pp. 519–523, 1976.

[13] A. J. Malan, L. Rausche, F. Strehle, and S. Hohmann, "Port-hamiltonian modelling for analysis and control of gas networks," *IFAC-PapersOnLine*, vol. 56, no. 2, pp. 5431–5437, 2023, 22nd IFAC World Congress.

[14] N. D. Manring and R. C. Fales, *Hydraulic Control Systems*. Wiley, 2019.

[15] J. Gravdahl, F. Willems, B. de Jager, and O. Egeland, "Modeling for surge control of centrifugal compressors: comparison with experiment," in *Proc. 39th IEEE Conf. Decis. Control (CDC)*, vol. 2, 2000, pp. 1341–1346.

[16] M. Arcak, C. Meissen, and A. Packard, *Networks of Dissipative Systems: Compositional Certification of Stability, Performance, and Safety*, ser. (SpringerBriefs in Control, Automation and Robotics). New York, NY, USA: Springer, 2016.

[17] J. W. Simpson-Porco, "Equilibrium-independent dissipativity with quadratic supply rates," *IEEE Trans. Autom. Control*, vol. 64, no. 4, pp. 1440–1455, 2019.

[18] A. J. van der Schaft, *L2-Gain and Passivity Techniques in Nonlinear Control*, 3rd ed. Cham: Springer, 2017.

[19] J. W. Simpson-Porco, Q. Shafiee, F. Dörfler, J. C. Vasquez, J. M. Guerrero, and F. Bullo, "Secondary frequency and voltage control of islanded microgrids via distributed averaging," *IEEE Trans. Ind. Electronics*, vol. 62, no. 11, pp. 7025–7038, 2015.

[20] R. T. Rockafellar and R. J. B. Wets, *Variational Analysis*. Berlin, Heidelberg: Springer, 1998.